Received: 28 March 2022 | Accepted: 9 September 2022

DOI: 10.1002/vzj2.20234

Vadose Zone Journal

ORIGINAL ARTICLE

Exploring the feasibility of using the soil temperature to identify preferential and lateral subsurface flows

Annelie Ehrhardt | **Horst H. Gerke**

Research Area 1 'Landscape Functioning', Working Group 'Hydropedology', Leibniz-Centre for Agricultural Landscape Research (ZALF), Eberswalder Straße 84, Müncheberg 15374, Germany

Correspondence
Annelie Ehrhardt, Research Area 1 'Landscape Functioning', Working Group 'Hydropedology', Leibniz-Centre for Agricultural Landscape Research (ZALF), Eberswalder Straße 84, Müncheberg, Germany, 15374.
Email: Annelie.Ehrhardt@zalf.de

Assigned to Associate Editor Joshua L. Heitman.

Funding information
Deutsche Forschungsgemeinschaft, Grant/Award Number: GE 990/13-1

Abstract

Soil temperature can be influenced by rapidly infiltrating water. Deviations from a uniform soil heat distribution could result from vertical preferential flow (VPF) and lateral subsurface flow (LSF) events. The objective was to identify the effect of infiltration on the soil temperature time series in a lysimeter with forced vertical movement and that in a sloping field to distinguish between VPF and LSF. Wavelet coherence analysis (WCA) was used to analyze soil temperature time series measured in a Colluvic Regosol close to the surface (15-cm depth) and below (80-cm depth) in a horizon with possible LSF occurrence. The soil temperatures in these depths were correlated at a daily scale reflecting diurnal fluctuations of air temperatures. A correlation at a monthly scale was similar to the periodicity in the wavelet spectrum of the precipitation from May through October 2015. In this period, soil temperatures at 80-cm depth changed faster in the lysimeter than in the field, indicating a dominating infiltration-induced vertical heat movement in the lysimeter. When assuming a temperature-dampening effect in the sloping field soil by laterally moving temperature-equilibrated soil water, observed deviations in soil temperature profiles between lysimeter and field could be indicative for LSF in the field. However, LSF occurrence could only be verified by soil water content measurements for single rainfall events in October and May. The analysis was useful to identify qualitatively relevant events in a time series. For quantitative analysis, soil moisture data need to be considered.

1 | INTRODUCTION

The processes of vertical preferential flow (VPF) and lateral subsurface flow (LSF) represent important pathways for water, nutrients, and pesticides in agricultural landscapes (e.g., Ritsema et al., 1996; Peyrard et al., 2016; Julich et al., 2017; Cueff et al., 2020). While VPF describes the gravity-driven rapid downward movement of infiltrating water in vertical cracks and biopores thereby bypassing large portions of a porous soil matrix (Gerke et al., 2010; Guo & Lin, 2018), the LSF denotes the lateral redirection of soil water along impeding layers or textural boundaries in sloping landscapes (Hendrickx & Flury, 2001; Jarvis et al., 2016). The identification of these flow patterns is still most essential for better quantitative understanding and predicting transport

Abbreviations: K_h, lateral hydraulic conductivity; K_v, vertical hydraulic conductivity; LSF, lateral subsurface flow; VPF, vertical preferential flow; WCA, wavelet coherence analysis; WTC, wavelet coherence spectra.

processes in soils (Vereecken et al., 2016; Hu et al., 2017; Lee & Kim, 2019).

Since VPF and LSF occur mostly irregularly on the basis of infrequent events, it is necessary to analyze longer-term continuous sets of soil moisture or tension data (Lin et al., 2006). Continuity of data time series is often impeded such as in case of tensions by soil drying or in general by sensor or logger failures (Ehrhardt et al., 2021). Smaller discontinuities may be corrected by gap-filling procedures (Groh et al., 2020); however, larger periods without data can only be reconstructed in a predictive way by simulations using a validated model (e.g., suction cup data; Weihermüller et al., 2011). In contrast to tensiometer data, soil temperature is more easily recorded and less prone to sensor failures (Partington et al., 2021). Thus, quasicontinuous time series of soil temperature data could be used to identify deviations from uniform flow patterns by making assumptions for the relationship between soil temperature and water flow.

Infiltrating water in soils can lead to a decrease in soil temperature in summer when the precipitation is cooler than the soil (Tang et al., 2003; Tao et al., 2017; Zhang et al., 2019). However, the soil can be cooler than the precipitation in winter such that infiltrating water from rain or snowmelt may lead to an increase in soil temperature (Yang et al., 2018); even thawing of permafrost soils has been attributed to the effect of water infiltration (Li et al., 2019). For unfrozen sloped soils, a soil temperature increase associated with infiltration was observed (Yoshioka et al., 2015; Sakura, 1984). Soil temperature as an indicator for water flow processes in the soil beneath riverbeds has been reported by Constantz et al. (2001) and Partington et al. (2021). These authors found interruptions in the daily soil temperature cycle during water flow events in nonperennial streams comparable to saturated infiltration into an agricultural soil.

Field observations confirmed theoretical considerations that LSF can only occur when the soil approaches water saturation, for example, because of impeding layers in the subsurface (Wöhling et al., 2012; Lin et al., 2006). Soil water saturation might also happen locally if a macropore transports water because of vertical preferential infiltration to the compacted layer in the subsurface (Guertault & Fox, 2020), and thus, local saturation is induced that leads to LSF (e.g., Newman et al., 2004). To detect LSF, one idea was to compare time series of soil moisture data in a lysimeter soil monolith with those of the same soil profile in the field at the extraction position; while in the lysimeter soil, flow is forced toward the vertical direction by the confining walls and the field soil water can move freely in all directions. This experimental system has been described before (Ehrhardt et al., 2021). The cored holes resulting from the extraction of a lysimeter soil monolith (i.e., 1-m diam., 1.5-m depth) were equipped with soil water content, matrix potential and temperature sensors in the same horizons as in the lysimeter. The lysimeters were re-established close to the field soil profiles and exposed to the same climatic conditions. The wavelet-based analysis of data from such a field–lysimeter set-up located in a hummocky ground moraine soil landscape (Sommer et al., 2016) indicated field–lysimeter deviations in water content time series in response to precipitation (Ehrhardt et al., 2021). With respect to LSF, the analysis of the soil water content time series suggested that faster increases in water content in the field vs. the lysimeter soil might indicate such LSF events in the horizon above the impeding layer. However, because of sensor failures, data could not be evaluated for a longer period. Data analysis of a longer time series might reveal the occurrence of LSF events at higher scales (e.g., annual or monthly scale).

Several possibilities of VPF and LSF effects on soil temperature can be considered (Figure 1): LSF is assumed to attenuate the warming or cooling effect of the infiltrating water. When the soil is cooler than the infiltrating water and infiltration is warming up the soil (e.g., Yang et al., 2018), water flowing laterally has a temperature in equilibrium with the surrounding soil temperature; here, LSF leads to an attenuation of the warming effect of the infiltrating water at the field site. Thus, the soil temperature in the lysimeter will increase faster than the soil in the field site since no LSF can enter the lysimeter (Figure 1a). In summer, the attenuation effect of LSF on soil temperature is similar, however, reversed in that the infiltrating precipitation leads to a cooling of the soil (Figure 1b) (cf., Zhang et al., 2019).

One major challenge for correlation analyses of time series is dealing with periodic fluctuations at divergent diurnal or seasonal cycles (e.g., Ding et al., 2013; Rahmati et al., 2020) especially with respect to soil temperature (Anctil et al., 2008). Classical measures of correlation, like Pearson correlation, only give a general estimate about the similarity of two time series while they do not account for temporal and scale variability within these time series (e.g., Bravo et al., 2020). A positive fluctuation of one time series might be superimposed by a negative fluctuation of the second time series, thus leading to a neutralization of positive and negative correlations (Biswas & Si, 2011). Wavelet

Core Ideas

- Diurnal soil temperature changes with wavelet coherence analysis (WCA) were detected.
- Temperature changes with depth are disrupted by precipitation and infiltration.
- Possible lateral subsurface flow (LSF) was identified.
- Soil moisture data was required for verification of detected LSF events by WCA.

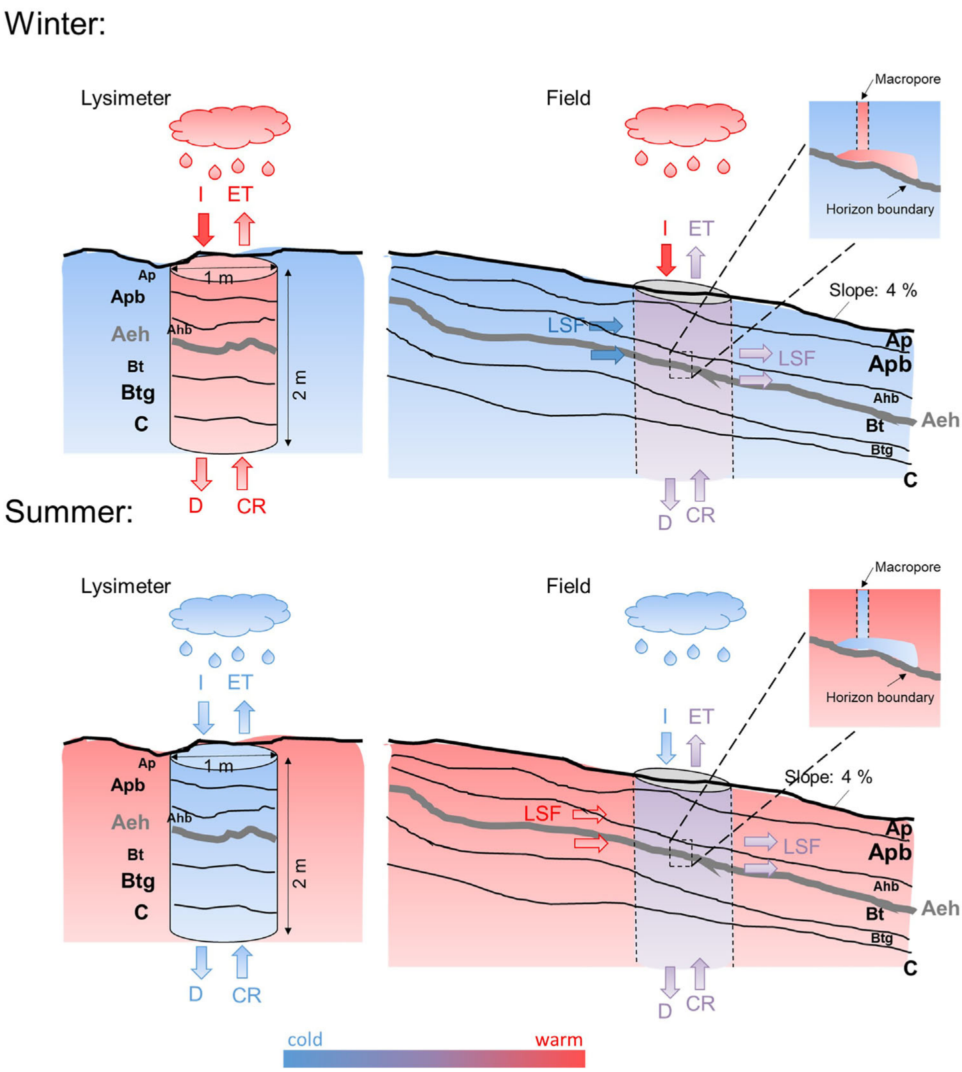

FIGURE 1 Concept of precipitation effect on soil temperature in winter and summer in the lysimeter and in the field. The influence of preferential flow in soil macropores is shown in the field plot but can also be applied to the lysimeter soil. Horizons (Ap, Apb, Ahb, Aeh, Bt, Btg, C) are named according to Ehrhardt et al. (2021). I, infiltration; ET, evapotranspiration; D, drainage; CR, capillary rise; LSF, lateral subsurface flow

coherence analysis (WCA) can be applied (Grinsted et al., 2004) to account for this temporal and scale variability when correlating two nonstationary and periodic time series. The WCA is a tool that can be compared with R^2 in a regression analysis (Si, 2008) and that correlates the wavelet spectra of two time series. Thus, information about dominant frequencies occurring within two time series can be extracted and correlated at every point of time (Gao & Yan 2011). Also, the phase shift between the two time series can be calculated. Thus, we hypothesize that anomalies in the correlation of two temperature time series from a lysimeter and a corresponding field site located at a slope position might help to identify LSF where data on soil hydraulic parameters that help to identify VPF and LSF are missing.

Then the objectives of the current paper are (a) to quantify the influence of infiltration events on the changes and depth shifts of soil temperatures with the WCA method by correlation indices and phase shift calculation and (b) to provide evidence that during infiltration events temporal shifts between lysimeter and field in the relation of temperature changes between smaller and greater soil depths exist. This is achieved by presenting typical correlation patterns and periods of temperature time series and deviations from these patterns that might be attributed to LSF.

2 | MATERIALS AND METHODS

2.1 | Study site, soil description, and measurement set-up

The study site ‘CarboZALF-D’ of the Leibniz-Centre for Agricultural Landscape Research (ZALF), Müncheberg (Sommer et al., 2016), is in northeastern Germany near the village of Holzendorf (53°23′ N, 13°47′ E; 50–60 m asl), a landscape dominated by hummocky ground moraines. Soil temperature data were collected in a lysimeter and a corresponding field profile at the position where the lysimeter was extracted (Figure 1). The soil is characterized as an Endogleyic Colluvic Regosol (IUSS Working Group WRB, 2006) with colluvic material from upper slope positions covering a former Luvisol to a depth of 70 cm. Lateral subsurface flow is expected to occur in the former A-horizon of the Luvisol (fAh-horizon) in ∼80-cm depth, since the vertical and lateral hydraulic conductivity (K_v and K_h) near saturation (pressure head $h = -1$ cm) are higher in the fAh-horizon (K_v = 14.4 cm d^{-1}, K_h = 23.7 cm d^{-1}) than in the horizons below (K_v = 0.7 cm d^{-1}, K_h = 1.0 cm d^{-1}). The values of K_v and K_h decrease with depth possibly because of a more compacted soil structure induced by the mass of the soil above or because of a lateral macropore network in the upper layers that is not present in the deeper horizons. In the present study, the same experimental set-up and the same soil are used as described in Ehrhardt et al. (2021). For detailed descriptions of the soils, the study site (e.g., climate data), and positions of the lysimeter and field profile, refer to Sommer et al. (2016) and Ehrhardt et al. (2021).

Soil temperature sensors (SM300, UGT, accuracy, ±0.5 °C; measurement range, 0–40 °C) were combined with a frequency domain reflectometry device for measuring the water content. They were installed at 15-, 32-, 60-, 85, 140-, and 190-cm depths in the lysimeter and at 15-, 32-, 55-, 80-, 140-, and 195-cm depths in the field profile. The sensor installation depth in the lysimeter and field soil varied because of local differences in the soil horizon boundary depths. The sensors were installed in the middle of each horizon so that no other horizon was accidentally instrumented. In the lysimeter, two sensors were inserted to a depth of 60 cm in each layer, whereas in the field profile, three sensors were inserted to a depth of 140 cm. In deeper horizons, only one sensor took temperature readings. Temperature was recorded with the data logger DL-2000 (Umwelt-Geräte-Technik GmbH) at 1-h intervals. For further details and a sketch on the sensor positions refer to Ehrhardt et al. (2021). Precipitation was recorded by five different types of rain gauges distributed across the CarboZALF-D experimental site (Supplemental Figure S1; Ehrhardt et al. 2021), manually corrected for outliers, and averaged in 1-h intervals. In 2015, a precipitation total of 474 mm was recorded.

2.2 | Data preparation and wavelet coherence analysis

Since the time series contained data gaps because of sensor or logger failures, data were reconstructed according to the gap filling procedure and data quality assessment as described in Ehrhardt et al. (2021).

For the WCA, the complex Morlet wavelet (wavenumber k_0 = 6) was chosen because of its good balance of time and frequency resolution (Grinsted et al., 2004). The statistical significance of the individual wavelet spectra was tested against a 'red-noise' background spectrum representing a first-order autoregressive process. A significance level of 5% against this background spectrum was chosen, and 300 Monte Carlo simulations were conducted to find the region of significant periods. A boxcar window was applied for wavelet smoothing. The calculation of the WCA spectra was carried out in MATLAB (release R2018a) (The MathWorks, Inc. 2019) using a MATLAB script provided by Hu and Si (2016) based on a MATLAB code developed by A. Grinsted (http://www.glaciology.net/wavelet-coherence). Global wavelet spectra representing the average power at a certain scale over the complete period was extracted in the R software v.3.6.2(R Core Team, 2019) using the package WaveletComp (Roesch & Schmidbauer, 2018). For further details on wavelet analysis and WCA refer to Si and Zeleke (2005) and Grinsted et al. (2004).

The variables used for WCA are the soil temperatures at 15- and 80-cm depth in the lysimeter and on field soil and hourly precipitation. The time series of soil temperature at 15-cm depth was the base signal and soil temperatures at 80-cm depth was the second signal. In case of the correlation between precipitation and soil temperature, precipitation was used the base signal and temperature as the second signal. Data were recorded at time intervals of 1 h. The period from 1 Jan. 2015 to 31 Dec. 2015 was analyzed.

2.3 | Phase shift analysis

Two time series might contain similar periodic fluctuations that are shifted in time against each other, for example, when soil temperature in a profile increases faster closer to the surface than in deeper layers. The information about the phase shift of two time series at a certain moment in time that are analyzed by WCA is given by the phase angle (Grinsted et al., 2004), represented by the arrows in a WCA plot. The phase angle φ_{xy} between a time series x and a time series y is derived from the imaginary (Im) and the real (Re) part of the smoothed cross-wavelet spectrum $\bar{S}_{x,y}$ (Si, 2008):

$$\varphi_{xy} = \arctan\left[\frac{\mathrm{Im}\left(\bar{S}_{x,y}\right)}{\mathrm{Re}\left(\bar{S}_{x,y}\right)}\right] \quad (1)$$

The phase shift at a certain period can also be converted into a time phase in hours for a certain scale. The phase angle is given in radians in the range from $-\pi$ to $+\pi$ (Roesch & Schmidbauer, 2018). At the 24-h scale, π corresponds to phase

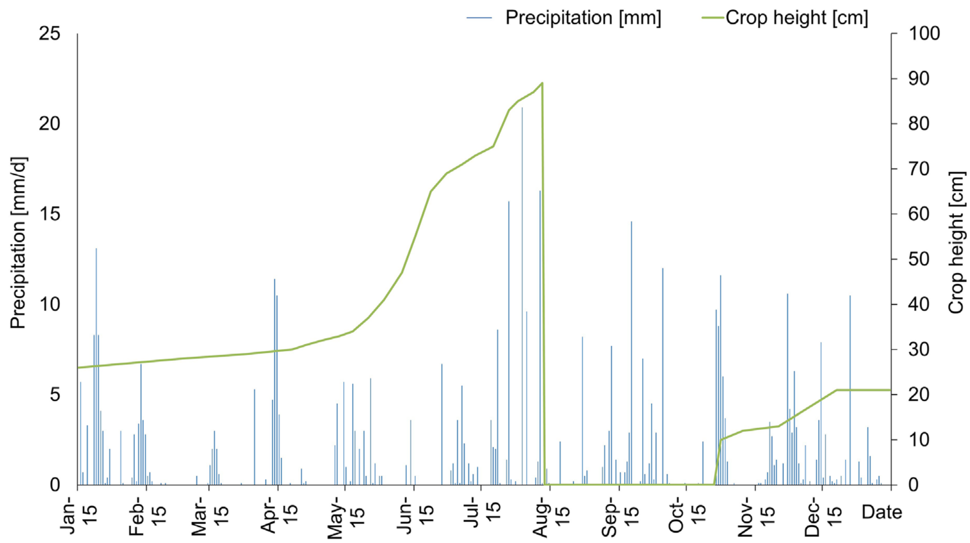

FIGURE 2 Crop height (cm) of winter wheat (green line) and precipitation (mm d^{-1}) in the year 2015

difference of 12 h (at the monthly scale, 1,024 h), π corresponds to a time lag of 512 h. For the phase shift analysis, the R package WaveletComp (Roesch & Schmidbauer, 2018) was applied to the original measurement data.

2.4 | Timing of field work and precipitation

The development of the winter wheat (*Triticum aestivum* L.) crop (Figure 2) was recorded three to four times a month by measuring the vertical crop height from the soil surface to the plant manually with a folding meter stick (Verch, ZALF Dedelow). Identical soil cultivation and crop management practices were carried out in the field plot and the lysimeter (Supplemental Table S1). Precipitation periods during the winter lasted for a few days with smaller rainfall amounts, whereas in summer, a higher total amount of rainfall was observed during a single day (Figure 2). Rainfall periods with a larger precipitation here occurred in the beginning of January and February, the beginning of April, the middle and end of July, the middle of September and October, and the middle of November (Figure 2). The crop height increased from ~30 cm at the beginning of May to 90 cm until the harvest at the end of July (Figure 2); then the soil remained bare until the new winter wheat crop started to grow in the middle of October.

3 | RESULTS

3.1 | Soil temperatures at 15- and 80-cm depth in lysimeter and field

Lateral subsurface flow is hypothesized to occur in the Ahb-horizon, so soil temperatures were analyzed at 80-cm depth and close to the surface at 15-cm depth as a reference to surface temperature. The lysimeter and the field soil temperatures show a strong seasonal pattern with warmer temperatures in summer and temperatures close to 0 °C in winter (Figure 3). At 15-cm depth, a strong diurnal cycle is observed. The temperature changes are smaller in winter (November through February) at both depths. Precipitation in winter leads to an overall increase in soil temperature as visible in the time series in January and December in Figure 3 and in the direct temperature response after the precipitation as found in Figure 4 and Supplemental Figure S1a. In late spring, summer, or early fall, a decrease in soil temperature is observed after precipitation (Figure 3; Supplemental Figure S1b), for example, in early June, in middle July (until beginning of August), and in early September (Figure 3; Supplemental Figure S1a).

At the end of July, a strong increase of diurnal temperature variations is observed especially at 15-cm depth in the lysimeter and the field (Figure 3). A similar but not so pronounced increase in diurnal temperature variations is observed in spring (Figure 3). In the field soil (Figure 3b) a higher maximum temperatures and larger daily amplitudes are observed at 15-cm depth compared with the lysimeter soil (Figure 3a). In contrast, the maximum temperature at 80-cm depth is smaller in the field soil than the lysimeter.

There was almost no difference in the dry mass of the straw and the grain yield between the lysimeter and the field after the harvest of winter wheat in summer 2015. In the lysimeter, a dry mass of the straw of 1.05 kg m^{-2} was found, whereas in the field, the dry mass of the straw amounted to 1.06 kg m^{-2}. The dry mass of the grain yield was 0.69 and 0.71 kg m^{-2} in the lysimeter and field, respectively. Thus, differences in soil temperature changes in lysimeter and field cannot be attributed to differing vegetation development in these plots.

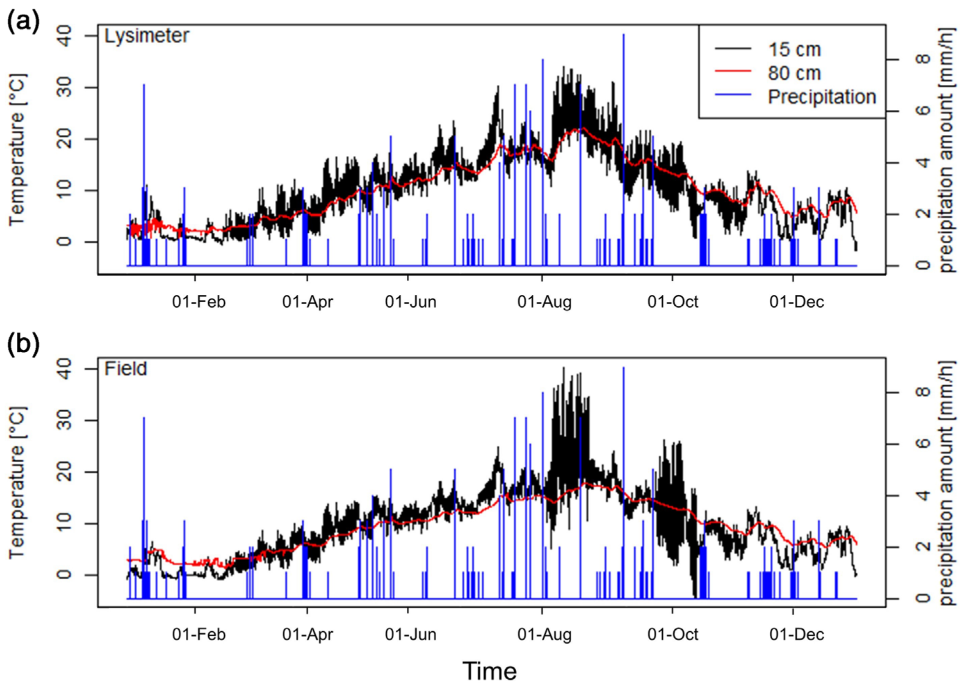

FIGURE 3 Time series of precipitation (mm h^{-1}) and soil temperature (°C) at 15- and 80-cm depth in the (a) lysimeter and (b) field soil in 2015

3.2 | Correlations of temperature changes between 15- and 80-cm depth

Wavelet spectra of the soil temperatures in the lysimeter and field show a pronounced diurnal (period = 24 h) pattern at 15-cm depth from early spring to late fall (Figure 5a,c). This daily pattern is also observed in the coherence spectra (wavelet coherence spectra [WTC] plots; Figure 5b,d) reflecting the correlation of soil temperatures between 15- and 80-cm depth. The WTC spectrum of the lysimeter seems to show more significant periods with correlations between those two depths than the field (Figure 5b,d). This is supported by the average cross-wavelet power at the 24-h scale being higher for the lysimeter than the field (Figure 6a). The average cross-wavelet power is gained when the cross-wavelet power (nonnormalized product of the wavelet spectra of two time series at one scale; Si & Zeleke, 2005; Cazelles et al., 2008) is averaged over the whole observed period at certain scales. Thus, the average correlation of soil temperature between 15- and 80-cm depth in the lysimeter and in the field soil can be compared.

At the 24-h scale, the phase shift in the lysimeter indicates anticorrelation. This means that temperatures at 15- and 80-cm are negatively correlated with each other with a complete lagging period (12 h).

At the monthly scale (period 512–1,024 h), significant deviations from the background spectrum are found from July to the end of the year in the lysimeter and the field soil at 80-cm depth (Figure 5a,c). In the correlation between the two examined depths, this period appears to be significant as well (Figure 5b,d). The phase shift in temperature change at 15- and 80-cm depth (indicated by the little black arrows in Figure 5b,d as well as by the phase shift expressed in hours in Figure 6b) is greater in the field soil than in the lysimeter (red circles in Figure 5). The phase shift is positive and larger for field than lysimeter during the significant correlation time interval at a monthly scale and corresponds approximately to a time lag of 170 h or 7 d (Figure 6b). A possible interpretation is that temperature changes occurring at a monthly period at 15-cm depth will be transferred to 80-cm depth with a time lag of 7 d. The phase shift between the lower and the upper depths remained relatively constant at a monthly scale. The phase shift difference at 80-cm is also found when the time series of lysimeter and field soil are directly correlated (Supplemental Figure S2). The arrows indicating the phase shift between lysimeter and field point slightly downwards between June and October at 80-cm depth, whereas at 15-cm depth, the arrows point to the right indicating no phase shift.

The daily pattern observed at the 24-h periodicity in the wavelet and wavelet coherence spectra (Figure 5) shows interruptions when the wavelet coherence spectra are calculated for a shorter period for 2 wk around major precipitation events (Figure 7; Table 1). For the detailed analysis, precipitation events with the highest recorded rainfall amount and peak intensity were chosen. The temperature correlations between 15- and 80-cm depth show a decrease in correlation during and after the rainfall for all events in the field (Figure 7b,d,f,h)

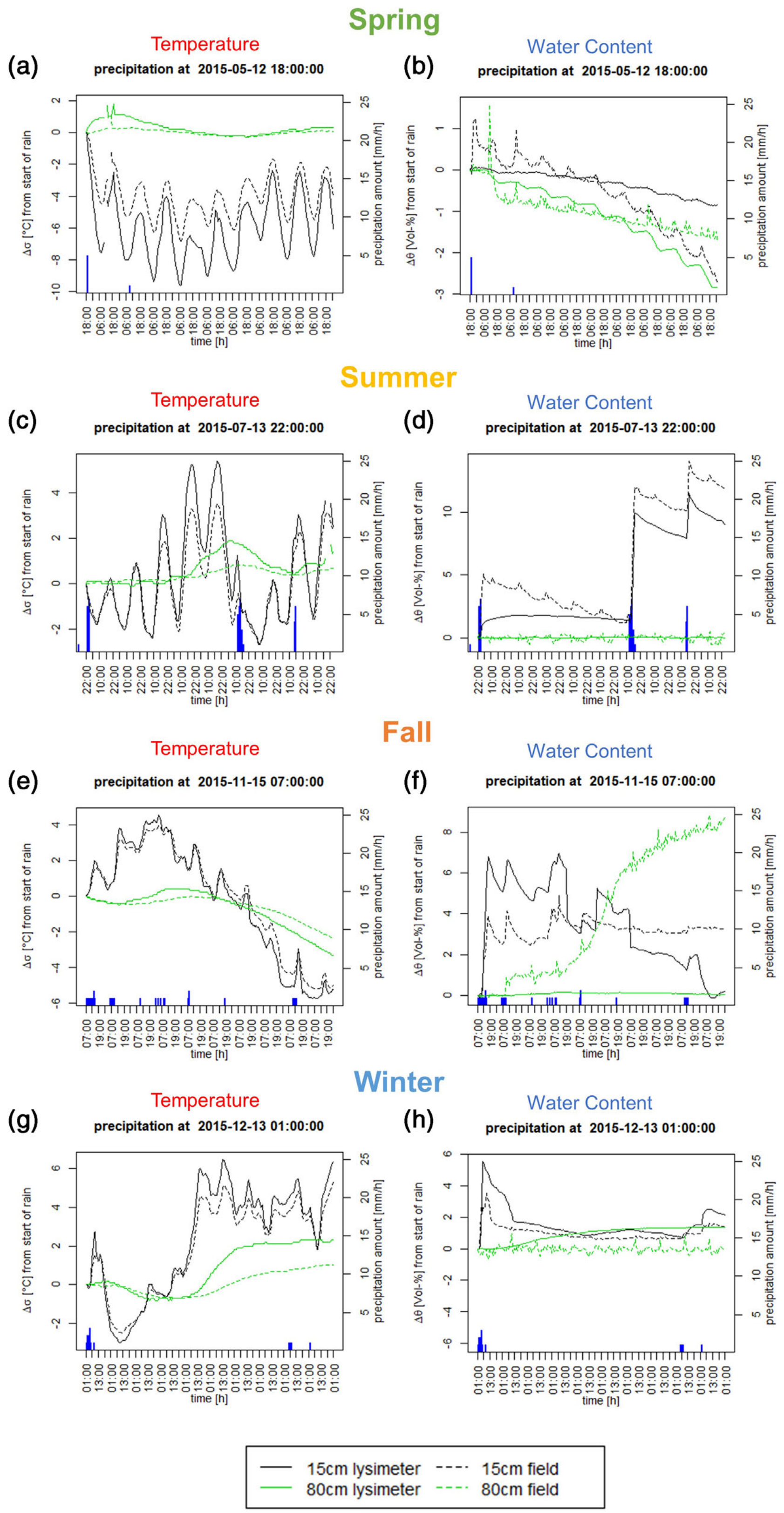

FIGURE 4 (a, c, e, g) Soil temperature and (b, d, f, h) soil water content change at 15- and 80-cm depth in the lysimeter and field after four precipitation events in spring, summer, fall, and winter. Soil temperature and soil water content changes were calculated as the difference to the soil temperature or water content before the rainfall event for each point in time. Precipitation amount in millimeters per hour is given on the right axes

and for the events in October and November in the lysimeter (Figure 7e,g) at the 24-h scale.

To analyze the effect of rainfall amount on the temperature patterns at daily and monthly scale, the wavelet coherence between the temperatures at 15- and 80-cm depth was averaged over different amounts of hourly rainfall (Figure 8). An overall increase of wavelet coherence is found with increasing rainfall intensity at the daily (24 h) and monthly scale. The

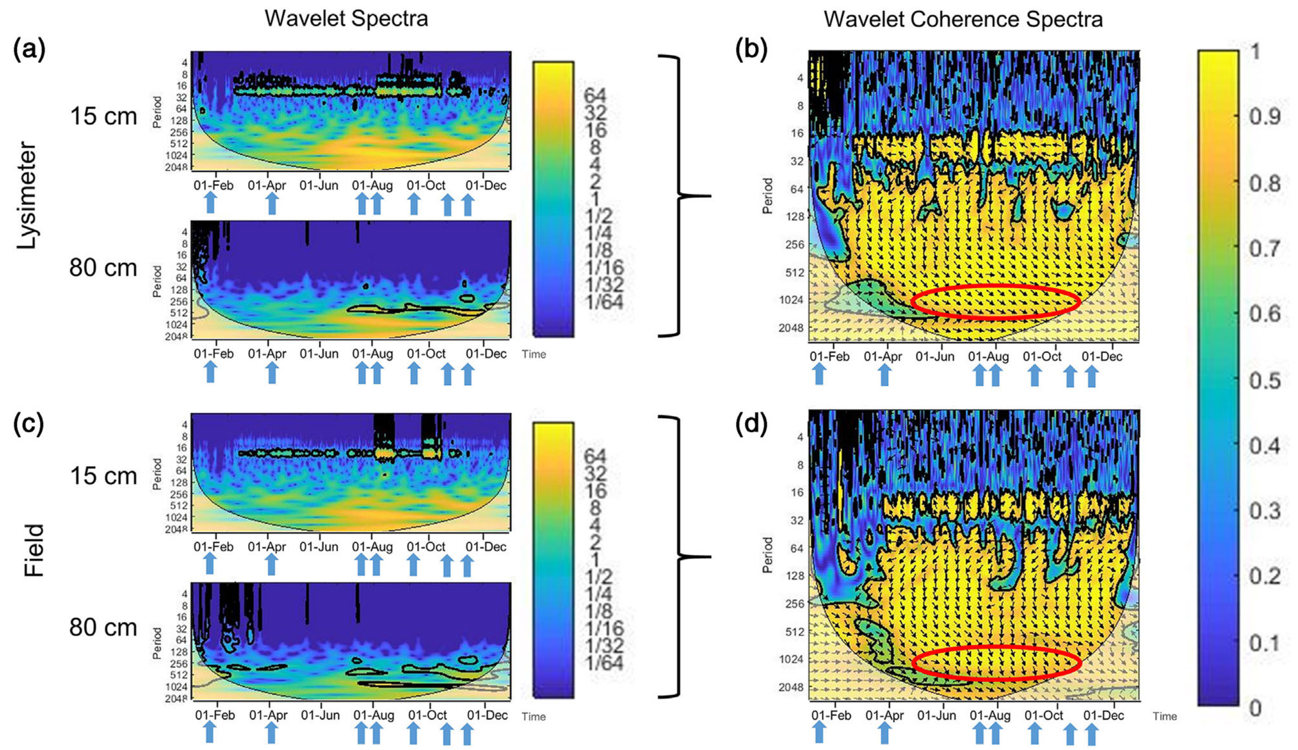

FIGURE 5 (a, c) Wavelet spectra and (b, d) wavelet coherence spectra depicting the correlation between 15- and 80-cm depth in the (a, b) lysimeter and the (c, d) field soil with the time given at the *x* axis and the periodicity in hours at the *y* axis. The base signal is the soil temperature at 15-cm depth and the second signal is the soil temperature at 80-cm depth. Significant deviations from the red noise background spectrum are surrounded by a black line. Areas outside the cone of influence (areas that should not be interpreted because of edge effects) are shaded. Phase shifts in temperature change between the time series of the upper and the lower soil depths are indicated by the little black arrows in the wavelet coherence spectra (WTC) plots. Arrows pointing to the right show perfect correlation (no phase shift), whereas arrows pointing left show anticorrelation. Arrows pointing downwards indicate that the time series of the upper soil horizon is ahead of the time series of the lower soil horizon. Blue arrows along the *x* axis indicate times of high precipitation amounts. The red circles in the plots highlight the correlations and phase shifts on a monthly scale

TABLE 1 Time, height, maximum intensity, and duration of precipitation events occurring in the time of significant periodicities in precipitation wavelet spectra and soil temperature wavelet coherence analysis spectra possibly indicating lateral subsurface flow

Date	Start time of rain event	Height	Maximum intensity	Duration
	h:min	mm	mm h^{-1}	h
13 June 2015	17:00	7	5	5
13 July 2015	22:00	13	7	2
19 July 2015	11:00	22	7	6
15 Aug. 2015	16:00	7	7	1
20 Sept. 2015	12:00	10	5	5
14 Oct. 2015	16:00	10	2	9
15 Nov. 2015	07:00	10	2	9

wavelet coherence does not differ much between the lysimeter and field at the monthly scale; however, some discrepancies are observed at the daily scale. For smaller rainfall events the coherence in the field is higher than in the lysimeter, whereas for larger rainfall events the coherence is higher in the lysimeter at a 24-h scale. The coherence is generally higher for the monthly scale than for the daily scale (Figure 8).

3.3 | Correlation between precipitation, soil temperature, and water content

The wavelet spectrum of the precipitation shows significant periodicities that deviate from the background spectrum at a monthly scale from the middle of June to the end of November (Figure 9a). In the wavelet coherence spectra of the

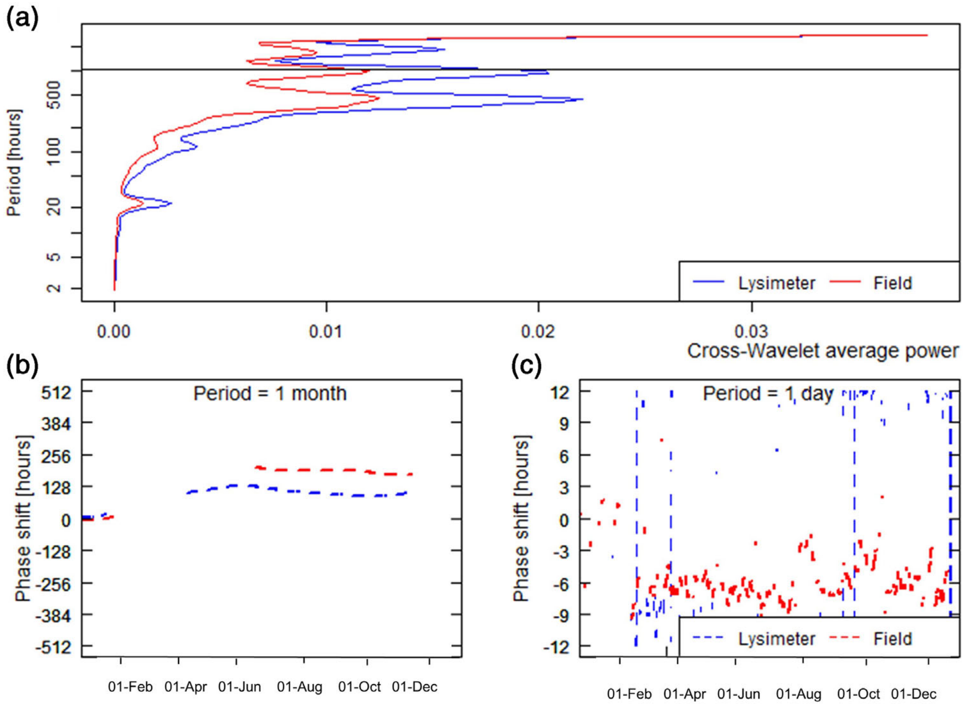

FIGURE 6 Cross-wavelet average power between 15- and 80-cm depth in the lysimeter and field soil. The black horizontal line indicates the monthly scale. (a) At the *y* axis, the periods are given at which the cross-wavelet power was averaged. Phase shift (hours) in soil temperature change between the upper (15 cm) and the lower depth (80 cm) in the lysimeter and field soil at the (b) monthly and (c) daily scale in the year 2015. A positive phase shift indicates a faster temperature change in the upper depth in comparison to the lower depth. The phase shift is given only in periods, where the wavelet coherence spectra deviate significantly from the background spectra

precipitation and the soil temperature at 15- and 80-cm depth in the lysimeter and the field, a significant correlation is found at the monthly scale (red circled areas in Figure 9b–e). Similar monthly correlation patterns were also found when correlating air temperature with the soil temperature (Supplemental Figure S3) and the water content with the soil temperature (Supplemental Figure S4).

Precipitation events occurring at a monthly scale in the period from June to the end of November are listed in Table 1. It includes all precipitation events that might cause LSF derived from the WCA of temperature and precipitation time series (Figure 9).

When analyzing soil temperature and water content changes in direct response to the infiltration events (Table 1) only for few events, soil temperature changes in lysimeter or field are accompanied by simultaneous water content changes. For example, an increase in temperature in the lysimeter and field at 80-cm depth is observed a few hours after the precipitation ceased on 12 May 2015 (Figure 4a). However, only in the field soil is an increase in water content found because of the infiltration event (Figure 4b). In later fall and early winter, an increase in temperature because of infiltrating water is observed at 80-cm depth especially for the lysimeter (Figure 4e,g). On 13 Dec. 2015, this temperature increase is reflected by a water content change in the lysimeter (Figure 4h). On 15 Nov. 2015 in the field soil, an increase in water content is found despite no temperature change at 80-cm depth (Figure 4e,f). In summer, the effect of cooling is observed at 80-cm depth after 22 mm of rainfall on 19 July 2015 (Figure 4c). Despite the temperature drop, no increase in water content is found in this horizon in the lysimeter and the field (Figure 4d). This phenomenon of temperature change after precipitation that is not accompanied by a change in water content is also found for other rainfall events in summer and early fall (Supplemental Figures S1a; Supplemental Figure S1b[b–f]).

4 | DISCUSSION

4.1 | Soil temperature variations with depth and season

Soil temperatures are affected by season and depend on soil depth. The strong diurnal cycle of the temperature time series in the lysimeter and field observed at 15-cm depth (Figures 3 and 4) is in correspondence with the findings of Anctil et al. (2008), Shanafield et al. (2017), and Tang et al. (2003). These authors observed stronger temperature variations in soil layers located closer to the surface than in deeper soil horizons.

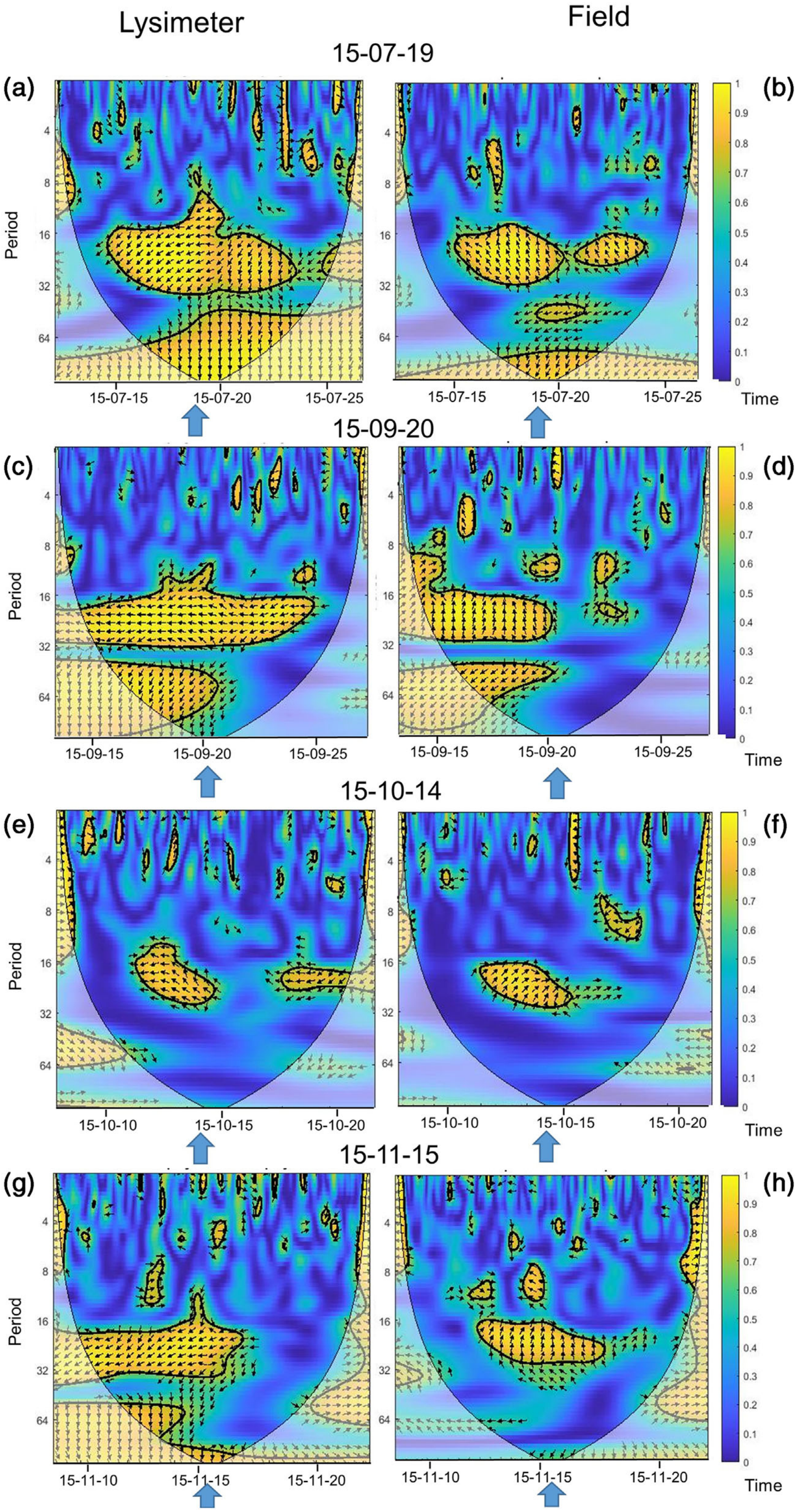

FIGURE 7 Wavelet coherence spectra depicting the correlation between 15- and 80-cm depth in the (a, c, e, g) lysimeter and the (b, d, f, h) field soil at four major precipitation events from July to November with the time given at the *x* axis and the periodicity in hours at the *y* axis. The base signal is the soil temperature at 15 cm depth and the second signal the soil temperature at 80 cm depth. The blue arrow indicates the start of the precipitation event

The increase in strong diurnal temperature variations at the end of July (Figure 3) could be attributed to the harvest of the winter wheat (Supplemental Table S1) since the missing vegetation cover cannot buffer the air temperatures anymore. This applies also to the increase in diurnal temperature fluctuations in spring (Figure 3) when the vegetation cover is still poorly developed.

An increasing phase shift between the upper and lower horizons as found in the WTC spectra (Figure 5b,d) has also been observed by Anctil et al. (2008) along with a damping of

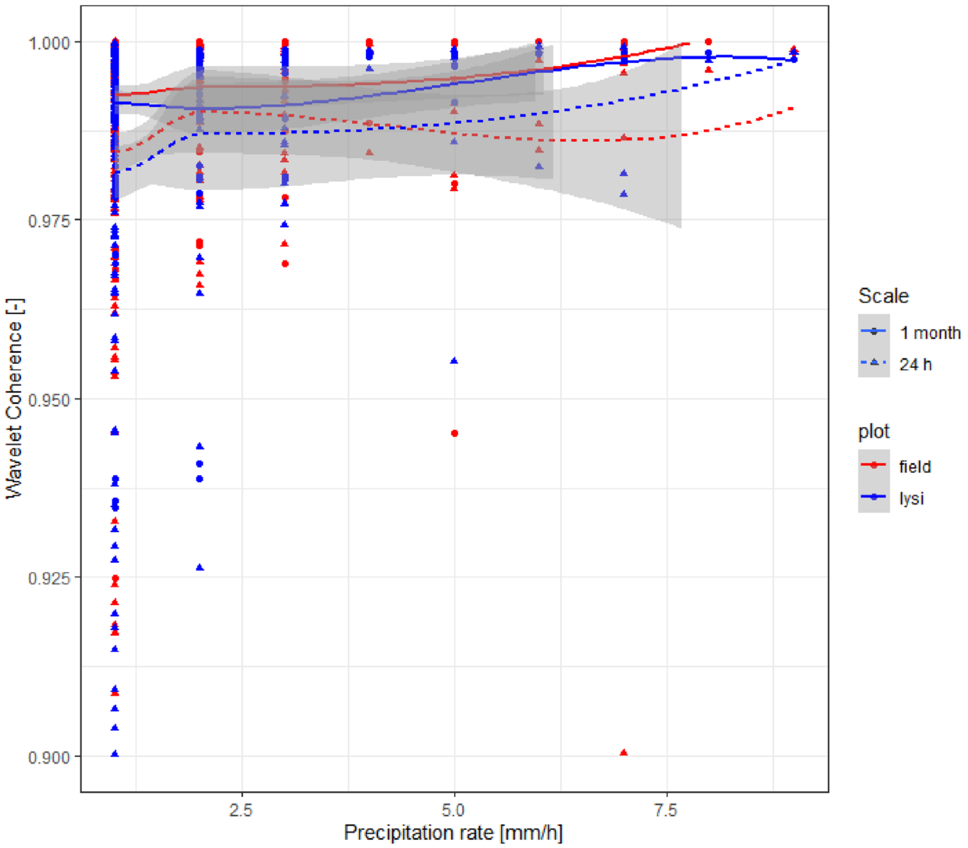

FIGURE 8 Average wavelet coherence in soil temperature change between the upper (15 cm) and the lower depth (80 cm) in the lysimeter (lysi) and field soil at different rates of precipitation at daily (24 h) and monthly (1 m) scale. Smoothing regression lines with confidence interval (grey areas) are calculated by local polynomial regression fitting

the wavelet signal. As in our study, the daily pattern in the soil temperature data disappeared in the wavelet spectra with increasing depth. Similar to this study (Figure 5b,d), Anctil et al. (2008) found an interruption of the diurnal temperature pattern in winter, which was attributed to the release of latent heat resulting from the freezing of the soil and an insulation effect of the snowpack.

4.2 | Effect of infiltration during precipitation periods on soil temperature

Warm winter rain leads to a warming of the soil in our study (Figure 4 a,g; Supplemental Figure S1a) as in the findings of Li et al. (2019) in permafrost soils. However, in early spring, summer, and early fall, a decrease in soil temperature after rainfall is observed (Figure 4c,e; Supplemental Figure S1a). This is in accordance with the soil temperature drops because of infiltration events found by Zhang et al. (2019) under Mediterranean climate conditions and Zhang et al. (2021) in the active layer of permafrost soils at the Central Tibet plateau. Tang et al. (2003) used this cooling effect of rainwater on a sand dune to deduce vertical infiltration velocities. In their experimental study in an eroded slope in China, Tao et al. (2017) could derive preferential flow patterns because of the cooling effect of summer rain on the soil. For example, they found a decrease in soil temperature at 80-cm depth accompanied by an increase in water content in the same layer before a change in water content or soil temperature was observed in layer above.

The effect of infiltration on soil temperature is also reflected in the absence of significant wavelet coefficients in the temperature time series in times of precipitation at a daily scale (Figure 7). This is in accordance with Constantz et al. (2001) and Partington et al. (2021), who found a damping effect in temperatures in the soil beneath the riverbed because of rainfall or streamflow events in nonperennial streams.

4.3 | Infiltration leads to different soil temperature depth correlations in the lysimeter and the field soil possibly indicating LSF

Periods with significant correlations in soil temperatures between 15-and 80-cm depth were more frequent in the coherence spectra of the lysimeter than in those of the field

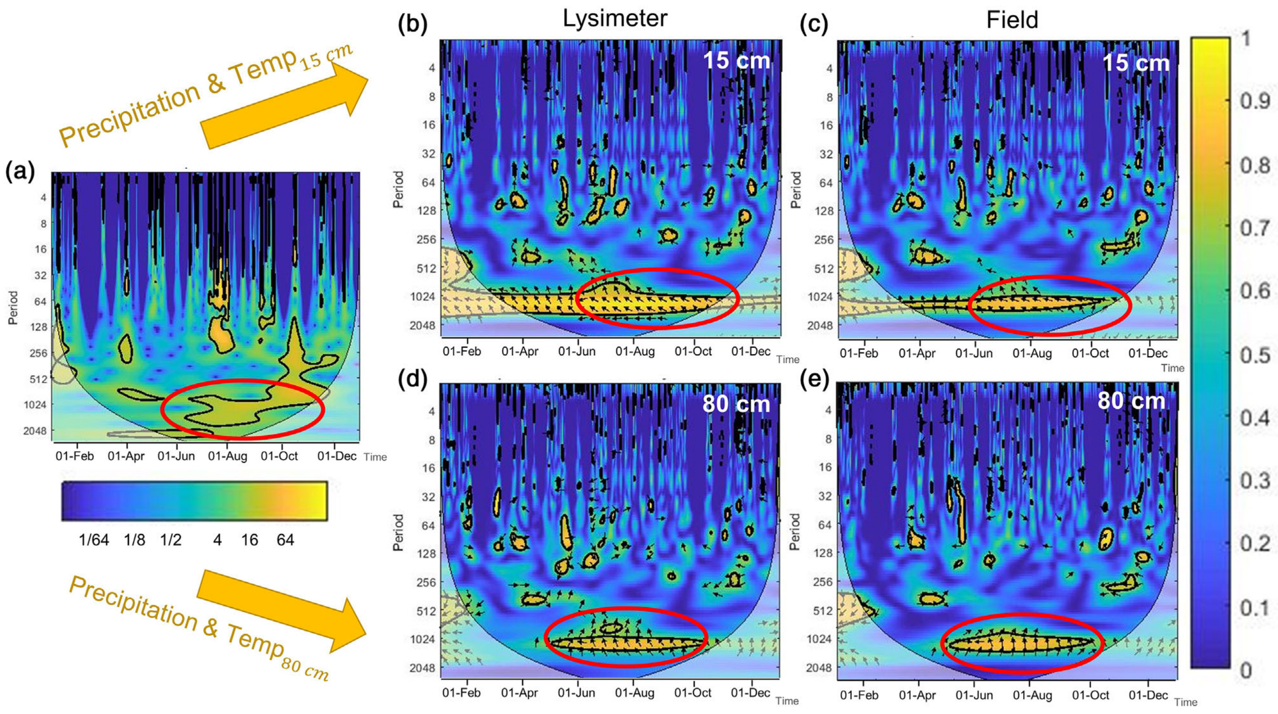

FIGURE 9 (a) Wavelet spectrum of the precipitation and the wavelet coherence spectra between precipitation and soil temperatures at (b, c) 15-cm depth and (d, e) 8- cm depth in lysimeter and field. The base signal is precipitation and the second signal the soil temperature. For a detailed description of the features visible in the individual plots refer to Figure 5. The red circles in the plots highlight the correlations and phase shifts on a monthly scale

(Figures 5b,d and 6a), indicating an enhanced vertical connectivity in the lysimeter compared with in the field. As in the conceptual model (Figure 1), water in the lysimeter moves only vertically. Thus, the temperature signal cannot be affected by LSF as in the field soil. This phase shift in temperature change between 15- and 80-cm depth is greater in the field than in the lysimeter (Figure 6b). In the field, water flowing laterally might delay the temperature increase at 80-cm depth by warming or cooling the soil water unless no VPF is present. Warmer water flowing laterally already adjusted to the soil temperatures in the field might mix with the cooler water from above and thus slow down the cooling of the deeper layers leading to a greater phase shift in the temperature propagation with depth. If VPF was present in the field, the differences between lysimeter and field would not be as pronounced, and the soil temperatures as well as the water contents would change simultaneously in the lysimeter and the field (Figure 1).

The theory of enhanced vertical connectivity also explains why correlations in soil temperature changes between 15- and 80-cm depth were found in the lysimeter but not for the field soil during the major precipitation events in July and September (Figure 7). The precipitation events on 19 July 2015 and 20 Sept. 2015 have the highest intensity of all events recorded in 2015 (Table 1). Thus, enhanced vertical flow in the lysimeter might have led to a fast temperature propagation from 15-cm depth to 80-cm depth leading to an enhanced coherence instead of an interruption of the coherence at the daily scale (Figures 5b and 7a,c).

The increase in wavelet coherence with increasing rainfall intensity indicates a better correlation between the temperature changes at 15- and 80-cm depth (Figure 8). This might be attributed to a larger water film connecting the pores and soil particles and thus enhancing the thermal conductivity (Jury & Horton, 2004) at larger precipitation events. Also, the average cross-wavelet power (Figure 6a) found in the lysimeter is a little bit higher than in the field soil and the wavelet coherence, especially for the 24-h scale during lager rainfall events (Figure 8), indicating a better vertical connectivity in the lysimeter soil. For smaller rainfall events (1–2 mm h^{-1}), the wavelet coherence between 15- and 80-cm depth is smaller than for larger precipitation rates at the daily scale (Figure 8). Such a phenomenon was observed by Zhang et al. (2021). In their study on the impact of summertime rainfall on the active layer in permafrost soils, it was found that lighter rainfall events have a minor impact on soil temperatures vs. larger rainfall events, which probably is due to preferential flow.

4.4 | Patterns at the monthly scale might indicate different subsurface flow processes in lysimeter and field soil

The direct influence of precipitation on soil temperatures can be derived in the following way. The wavelet spectrum of precipitation shows significant periodicities at the monthly scale from the middle of June to the end of November (Figure 9a), which is the same scale and period where soil temperature is correlated to precipitation (Figure 9b–d). Thus, soil temperature could be influenced by precipitation. From this it can be concluded that differences in soil temperature changes between lysimeter and field, shown by differing phase shifts between 15- and 80-cm depth at this monthly scale in the period from spring to fall, might be attributed to precipitation (Figure 5b,d). Throughout the winter, such correlation exists as well but cannot be interpreted since it lies outside the cone of influence (for explanation, see Figure 5). Taking these findings into account, the times of possible LSF occurrence were derived for major precipitation events in the time from June to the end of November 2015 (Table 1).

Note that the phase shift difference between the lysimeter and the field found at the monthly scale (Figure 6b) is different at the daily scale (Figures 5b,d and 6c). The phase shift between 15- and 80-cm depth is even more negatively correlated with a complete lag of 12 h for the lysimeter soil than for the field soil on the 24-h scale. This indicates a faster temperature change at 80-cm depth than in the upper layer (Figures 5b,d, 6c, and 7). It can only be explained if the temperature cycle of the previous day at 80-cm depth is closer correlated to the temperature cycle at 15-cm depth of the next day than the previous day. This leads to wrong interpretations of the daily phase shifts between soil temperature data of different depths, and thus, the interpretation of the daily phase shift of soil temperature data is not recommended. Also, the phase shifts at daily scale provide only a little information on the effect of rainfall infiltration on soil temperature since correlation ceases at this scale during precipitation (Figure 7). The stronger negative correlation in the field vs. in the lysimeter can be explained by the enhanced vertical connectivity of the lysimeter soil as already explained above.

4.5 | Verification of subsurface flow processes identified by soil temperatures with soil water content data necessary

If the observed temperature patterns are related to precipitation, than an influence of precipitation on the soil water content should be found. When comparing the change in soil water content to the change in the soil temperature at 15- and 80-cm depth in the lysimeter and the field directly after the precipitation events summarized in Table 1, especially in summer and early fall, almost no change in water content is observed at 80-cm depth after precipitation (Figure 4d; Supplemental Figure S1b[b–f]). Only in winter and spring are the faster soil temperature changes found in the lysimeter vs. In the field and are reflected by a faster water content increase in the lysimeter at 80-cm depth (Figure 4b,h). Thus, the patterns observed in the WCA plots of the temperature data over the summer and early fall period cannot be related to flow processes. The lack of water content increase at 80-cm depth in summer could be explained by a quick evaporation or root water uptake of the infiltrating water. The temperature changes observed in this period might be caused by an air temperature change induced by the precipitation or weather conditions. This would also explain the poor correlations found between water content and soil temperatures at 80-cm depth (Supplemental Figure S4).

Despite the lack of water flow occurrence or soil water content change in summer, LSF might be possible in spring and late fall. In spring, water content increase at 80-cm depth is found in the field after a precipitation event, which is not observed for the lysimeter soil (Figure 4b). However, no temperature change is found in the field soil, whereas the soil temperature in the lysimeter increases ~1 ˚C (Figure 4a). Water flowing laterally in the field might have caused this water content increase. Water flowing laterally in the field is already adjusted to the temperatures at 80-cm depth, therefore, no temperature change but only water content change is observed in the field soil. In later autumn (15 Nov. 2015), a similar pattern, possibly indicating LSF, is found; the temperature in the field soil does not increase at 80-cm depth (Figure 4e), whereas the water content rises by 8% volumetrically (Figure 4f) because of the infiltration events.

In winter, a VPF event might have occurred in the lysimeter according to Figure 1; on 13 Dec. 2015, the temperature as well as the water content increases in the lysimeter, which is not observed for the field soil (Figure 4 g,h). Water might have travelled through a macropore to the horizon boundary, thus leading to a faster increase in water content and soil temperature in the lysimeter than in the field soil (Guertault & Fox, 2020; Newman et al. 2004).

Thus, only in winter or late autumn could significant patterns be found in the wavelet spectra and wavelet coherence spectra of the soil temperature data that might be attributed to the influence of precipitation and subsurface water flow.

5 | CONCLUSIONS

Since soil temperatures might be easier to monitor and obtain with less technical problems than soil water contents or matric potentials, we wanted to test the possibility of identifying vertical (VPF) and lateral preferential flow (LSF) during infiltration events from soil temperature time series. The approach assumes VPF occurrence in the case of rapid soil temperatures changes in the greater soil depths during water infiltration that deviate from diurnal or annual fluctuations. An occurrence of LSF in sloping field soil horizons may be assumed if soil temperature changes in the greater depth deviate from those in the same horizon of a lysimeter soil without lateral flow. Information could be gained from temporal shifts in correlations of soil temperature changes between smaller and greater depths and between lysimeter and field during infiltration events obtained with WCA.

The results suggest that it is not advisable to use temperature data alone for the identification of flow processes in the subsurface. The WCA correlation indices and phase shifts of the temperature time series suggested that periods with LSF possibly occurred at a monthly scale for precipitation from June through November 2015. Confirmation of temperature identified LSF with water content data was possible for one event in November 2015 when the soil water content increased in the field at 80-cm depth but not in the lysimeter. In contrast, the possible LSF occurrence, according to the water content data, could not be identified by the WCA of the soil temperature data for an event in spring. The missing correlations of soil temperature changes with soil water dynamics after heavy summer precipitation events indicated that the temperature gradient in the rainwater and in the deeper soil did not deviate enough or that temperature changes in the deeper unsaturated soil systems were indeed in this period less connected through preferential flow with subsurface flow processes. Thus, the WCA analysis of soil temperature data can mainly be used to distinguish possible periods of LSF and needs to be verified by soil water content or tension data.

This test application showed the use and the limitations of the method for a relatively short period of time. To determine exactly at what times or under what boundary conditions temperature data can be used to indicate the occurrence of subsurface flow, additional time periods and other soil profiles must be analyzed. The conflicting results for events where LSF is expected to occur based on soil moisture data but not on temperature data suggest that the proposed method is less useful for highly unsaturated or variably saturated soil systems than for saturated soil systems. Wavelet coherence analysis of temperature data could be useful for identifying LSF events in late autumn to early spring during periods with higher soil moisture and snowmelt.

ACKNOWLEDGMENTS

This study was financially supported by the Deutsche Forschungsgemeinschaft (DFG), Bonn, Germany, under grants GE 990/13-1 'Vadose Zone Modelling of water flow in hillslope soil (VAMOS)'. The authors thank Dr. B. Si (University of Saskatchewan) and Dr. W. Hu (New Zealand Institute for Plant and Food Research Limited) for providing the MATLAB code for the wavelet transform and wavelet coherence analyses and further support with the implementation. We want to thank the reviewers and the editor for constructive comments and suggestions to improve the manuscript. We are grateful for the set-up and maintenance of the lysimeter and field profile by Prof. Dr. Hans-Jörg Vogel, Dr. Max Köhne and Robert Lüdtke (UFZ, Halle, Germany), and Nico Zindler (ZALF, Müncheberg). Gernot Verch (ZALF, Dedelow) is acknowledged for the crop height measurement.

AUTHOR CONTRIBUTIONS

Annelie Ehrhardt: Conceptualization; Data curation; Formal analysis; Investigation; Methodology; Resources; Software; Validation; Visualization; Writing-original draft; Writing-review & editing. Horst H. Gerke: Conceptualization; Funding acquisition; Investigation; Project administration; Resources; Supervision; Writing-review & editing.

CONFLICT OF INTEREST

The authors declare no conflicts of interest.

ORCID

Annelie Ehrhardt https://orcid.org/0000-0003-0512-4814
Horst H. Gerke https://orcid.org/0000-0002-6232-7688

REFERENCES

Anctil, F., Pratte, A., & Le Parent Bolinder, M. A. (2008). Non-stationary temporal characterization of the temperature profile of a soil exposed to frost in south-eastern Canada. *Nonlinear Processes in Geophysics*, *15*, 409–416.

Biswas, A., & Si, B. C. (2011). Identifying scale specific controls of soil water storage in a hummocky landscape using wavelet coherency. *Geoderma*, *165*, 50–59. https://doi.org/10.1016/j.geoderma.2011.07.002

Bravo, S., González-Chang, M., Dec, D., Valle, S., Wendroth, O., Zúñiga, F., & Dörner, J. (2020). Using wavelet analyses to identify temporal coherence in soil physical properties in a volcanic ash-derived soil. *Agricultural and Forest Meteorology*, *285–286*, 107909. https://doi.org/10.1016/j.agrformet.2020.107909

Cazelles, B., Chavez, M., Berteaux, D., Ménard, F., Vik, J. O., Jenouvrier, S., & Stenseth, N. C. (2008). Wavelet analysis of ecological time series. *Oecologia*, *156*, 287–304. https://doi.org/10.1007/s00442-008-0993-2

Constantz, J., Stonestorm, D., Stewart, A. E., Niswonger, R., & Smith, T. R. (2001). Analysis of streambed temperatures in ephemeral channels to determine streamflow frequency and duration. *Water Research*, *37*, 317–328.

Cueff, S., Alletto, L., Bourdat-Deschamps, M., Benoit, P., & Pot, V. (2020). Water and pesticide transfers in undisturbed soil columns sampled from a Stagnic Luvisol and a Vermic Umbrisol both cultivated under conventional and conservation agriculture. *Geoderma*, *377*, 114590. https://doi.org/10.1016/j.geoderma.2020.114590

Ding, R., Kang, S., Vargas, R., Zhang, Y., & Hao, X. (2013). Multiscale spectral analysis of temporal variability in evapotranspiration over irrigated cropland in an arid region. *Agricultural Water Management*, *130*, 79–89. https://doi.org/10.1016/j.agwat.2013.08.019

Ehrhardt, A., Groh, J., & Gerke, H. H. (2021). Wavelet analysis of soil water state variables for identification of lateral subsurface flow: Lysimeter vs. field data. *Vadose Zone Journal*, *20*, 149. https://doi.org/10.1002/vzj2.20129

Gao, R. X., & Yan, R. (2011). From Fourier transform to wavelet transform: A historical perspective. In *Wavelets* (pp. 17–32). Springer. https://doi.org/10.1007/978-1-4419-1545-0_2

Gerke, H. H., Germann, P., & Nieber, J. (2010). Preferential and unstable flow: From the pore to the catchment scale. *Vadose Zone Journal*, *9*, 207–212. https://doi.org/10.2136/vzj2010.0059

Grinsted, A., Moore, J. C., & Jevrejeva, S. (2004). Application of the cross wavelet transform and wavelet coherence to geophysical time series. *Nonlinear Processes in Geophysics*, *11*, 561–566.

Groh, J., Diamantopoulos, E., Duan, X., Ewert, F., Herbst, M., Holbak, M., Kamali, B., Kersebaum, K., Kuhnert, M., Lischeid, G., Nendel, C., Priesack, E., Steidl, J., Sommer, M., Pütz, T., Vereecken, H., Wallor, E., Weber, T. K. D., Wegehenkel, M., … Gerke, H. H. (2020). Crop growth and soil water fluxes at erosion-affected arable sites: Using weighing lysimeter data for model intercomparison. *Vadose Zone Journal*, *19*, e20058. https://doi.org/10.1002/vzj2.20058

Guertault, L., & Fox, G. A. (2020). Performance of preferential flow models in predicting infiltration through a remolded soil with artificial macropores. *Vadose Zone Journal*, *19*, e20055. https://doi.org/10.1002/vzj2.20055

Guo, L., & Lin, H. (2018). Addressing two bottlenecks to advance the understanding of preferential flow in soils. *Advances in Agronomy*, *147*, 61–117. https://doi.org/10.1016/bs.agron.2017.10.002

Hendrickx, J. M. H., & Flury, M. (2001). Uniform and preferential flow, mechanisms in the vadose zone. In *Conceptual models of flow and transport in the fractured vadose zone* (pp. 149–187). National Academy Press. https://nap.nationalacademies.org/read/10102/chapter/7#151

Hu, W., & Si, B. C. (2016). Technical note: Multiple wavelet coherence for untangling scale-specific and localized multivariate relationships in geosciences. *Hydrology and Earth System Sciences*, *20*, 3183–3191. https://doi.org/10.5194/hess-20-3183-2016

Hu, W., Si, B. C., Biswas, A., & Chau, H. W. (2017). Temporally stable patterns but seasonal dependent controls of soil water content: Evidence from wavelet analyses. *Hydrological Processes*, *31*, 3697–3707. https://doi.org/10.1002/hyp.11289

IUSS Working Group WRB (2006). *World reference base for soil resources 2006: A framework for international classification, correlation and communication* (World soil resources reports no. 103). FAO. https://wwwuser.gwdg.de/~kuzyakov/soilrus/wrb2006final.pdf

Jarvis, N., Koestel, J., & Larsbo, M. (2016). Understanding preferential flow in the vadose zone: Recent advances and future prospects. *Vadose Zone Journal*, *15*, 1–11. https://doi.org/10.2136/vzj2016.09.0075

Julich, D., Julich, S., & Feger, K.-H. (2017). Phosphorus fractions in preferential flow pathways and soil matrix in hillslope soils in the Thuringian Forest (Central Germany). *Journal of Plant Nutrition and Soil Science*, *180*, 407–417. https://doi.org/10.1002/jpln.201600305

Jury, W. A., & Horton, R. (2004). *Soil physics*. John Wiley & Sons.

Lee, E., & Kim, S. (2019). Wavelet analysis of soil moisture measurements for hillslope hydrological processes. *Journal of Hydrology*, *575*, 82–93. https://doi.org/10.1016/j.jhydrol.2019.05.023

Li, D.-S., Wen, Z., Cheng, Q.-G., Xing, A.-G., Zhang, M.-L., & Li, A.-Y. (2019). Thermal dynamics of the permafrost active layer under increased precipitation at the Qinghai-Tibet Plateau. *Journal of Mountain Science*, *16*, 309–322. https://doi.org/10.1007/s11629-018-5153-5

Lin, H., Kogelmann, W. J., Walker, C., Bruns, M., & Ann, V. (2006). Soil moisture patterns in a forested catchment: A hydropedological perspective. *Geoderma*, *131*, 345–368. https://doi.org/10.1016/j.geoderma.2005.03.013

The MathWorks, Inc. (2019). *MATLAB (Release R2018a)*. The MathWorks Inc.

Newman, B. D., Wilcox, B. P., & Graham, R. C. (2004). Snowmelt-driven macropore flow and soil saturation in a semiarid forest. *Hydrological Processes*, *18*, 1035–1042. https://doi.org/10.1002/hyp.5521

Partington, D., Shanafield, M., & Turnadge, C. (2021). A comparison of time-frequency signal processing methods for identifying non-perennial streamflow events from streambed surface temperature time series. *Water Research*, *57*, 632. https://doi.org/10.1029/2020WR028670

Peyrard, X., Liger, L., Guillemain, C., & Gouy, V. (2016). A trench study to assess transfer of pesticides in subsurface lateral flow for a soil with contrasting texture on a sloping vineyard in Beaujolais. *Environmental Science and Pollution Research*, *23*, 14–22. https://doi.org/10.1007/s11356-015-4917-5

Rahmati, M., Groh, J., Graf, A., Pütz, T., Vanderborght, J., & Vereecken, H. (2020). On the impact of increasing drought on the relationship between soil water content and evapotranspiration of a grassland. *Vadose Zone Journal*, *19*, e20029. https://doi.org/10.1002/vzj2.20029

R Core Team. (2019). *R: A language and environment for statistical computing* (Version R-3.6.2). R Foundation for Statistical Computing. https://www.R-project.org

Ritsema, C. J., Oostindie, K., & Stolte, J. (1996). Evaluation of vertical and lateral flow through agricultural loessial hillslopes using a two-dimensional computer simulation model. *Hydrological Processes*, *10*, 1091–1105. https://doi.org/10.1002/(sici)1099-1085(199608)10:8⟨1091::aid-hyp414⟩3.0.co;2-j

Roesch, A., & Schmidbauer, H. (2018). *WaveletComp: Computational wavelet analysis*. https://CRAN.R-project.org/package=WaveletComp

Sakura, Y. (1984). Change of thermal regime in surface soil layer during a heavy rain. (In Japanese with English abstract) *Geographical Review of Japan*, *57*, 628–638.

Si, B. C. (2008). Spatial scaling analyses of soil physical properties: A review of spectral and wavelet methods. *Vadose Zone Journal*, *7*, 547–562. https://doi.org/10.2136/vzj2007.0040

Si, B. C., & Zeleke, T. B. (2005). Wavelet coherency analysis to relate saturated hydraulic properties to soil physical properties. *Water Resources Research*, *41*, 395. https://doi.org/10.1029/2005WR004118

Shanafield, M., McCallum, J. L., Cook, P. G., & Noorduijn, S. (2017). Using basic metrics to analyze high-resolution temperature data in the subsurface. *Hydrogeology Journal*, *25*, 1501–1508. https://doi.org/10.1007/s10040-017-1578-0

Sommer, M., Augustin, J., & Kleber, M. (2016). Feedbacks of soil erosion on SOC patterns and carbon dynamics in agricultural landscapes—The CarboZALF experiment. *Soil and Tillage Research*, *156*, 182–184. https://doi.org/10.1016/j.still.2015.09.015

Tang, C., Shindo, S., Sakura, Y., & Machida, I. (2003). A possibility for tracing infiltration fronts by temperature in sand dunes: An experimental study. *Environmental Geology*, *44*, 169–175. https://doi.org/10.1007/s00254-002-0741-6

Tao, Y., He, Y., Duan, X., Zou, Z., Lin, L., & Chen, J. (2017). Preferential flows and soil moistures on a Benggang slope: Determined by the water and temperature co-monitoring. *Journal of Hydrology*, *553*, 678–690. https://doi.org/10.1016/j.jhydrol.2017.08.029

Vereecken, H., Pachepsky, Y., Simmer, C., Rihani, J. F., Kunoth, A., & Korres, W., Graf, A., Franssen, H. J.-H., Thiele-Eich, I., & Shao, Y. (2016). On the role of patterns in understanding the functioning of soil-vegetation-atmosphere systems. *Journal of Hydrology*, *542*, 63–86. https://doi.org/10.1016/j.jhydrol.2016.08.053

Weihermüller, L., Kasteel, R., Vanderborght, J., Šimůnek, J., & Vereecken, H. (2011). Uncertainty in pesticide monitoring using suction cups: Evidence from numerical simulations. *Vadose Zone Journal*, *10*, 1287–1298. https://doi.org/10.2136/vzj2011.0017

Wöhling, T., Bidwell, V. J., & Barkle, G. F. (2012). Dual-tracer, non-equilibrium mixing cell modelling and uncertainty analysis for unsaturated bromide and chloride transport. *Journal of Contaminant Hydrology*, *140–141*, 150–163. https://doi.org/10.1016/j.jconhyd.2012.08.001

Yang, Y., Wu, Z., He, H., Du, H., Wang, L., Guo, X., & Zhao, W. (2018). Differences of the changes in soil temperature of cold and mid-temperate zones, northeast China. *Theoretical and Applied Climatology*, *134*, 633–643. https://doi.org/10.1007/s00704-017-2297-0

Yoshioka, M., Takakura, S., Ishizawa, T., & Sakai, N. (2015). Temporal changes of soil temperature with soil water content in an embankment slope during controlled artificial rainfall experiments. *Journal of Applied Geophysics*, *114*, 134–145. https://doi.org/10.1016/j.jappgeo.2015.01.009

Zhang, M., Wen, Z., Li, D., Chou, Y., Zhou, Z., Zhou, F., & Lei, B. (2021). Impact process and mechanism of summertime rainfall on thermal-moisture regime of active layer in permafrost regions of central Qinghai-Tibet Plateau. *The Science of the Total Environment*, *796*, 148970. https://doi.org/10.1016/j.scitotenv.2021.148970

Zhang, S., Meurey, C., & Calvet, J.-C. (2019). Identification of soil-cooling rains in southern France from soil temperature and soil moisture observations. *Atmospheric Chemistry and Physics*, *19*, 5005–5020. https://doi.org/10.5194/acp-19-5005-2019

SUPPORTING INFORMATION

Additional supporting information can be found online in the Supporting Information section at the end of this article.

How to cite this article: Ehrhardt, A., & Gerke, H. H. (2023). Exploring the feasibility of using the soil temperature to identify preferential and lateral subsurface flows. *Vadose Zone Journal*, *22,* e20234. https://doi.org/10.1002/vzj2.20234